Tracer Testing for Estimating Heat Transfer Area in Fractured Reservoirs

Karsten Pruess[1], Ton van Heel[2], and Chao Shan[1]

1   Lawrence Berkeley National Laboratory, One Cyclotron Road, Berkeley, CA 94720, U.S.A.

2   Shell International Exploration and Production B.V., Volmerlaan 8, P.O. Box 60, 2280 AB Rijswijk, The Netherlands

K_Pruess@lbl.gov

ABSTRACT

A key parameter governing the performance and life-time of a Hot Fractured Rock (HFR) reservoir is the effective heat transfer area between the fracture network and the matrix rock. We report on numerical modeling studies into the feasibility of using tracer tests for estimating heat transfer area. More specifically, we discuss simulation results of a new HFR characterization method which uses *surface*-sorbing tracers for which the adsorbed tracer mass is proportional to the fracture surface area per unit volume. Sorption in the rock matrix is treated with the conventional formulation in which tracer adsorption is volume-based. A slug of solute tracer migrating along a fracture is subject to diffusion across the fracture walls into the adjacent rock matrix. Such diffusion removes some of the tracer from the fluid in the fractures, reducing and retarding the peak in the breakthrough curve (BTC) of the tracer. After the slug has passed the concentration gradient reverses, causing back-diffusion from the rock matrix into the fracture, and giving rise to a long tail in the BTC of the solute. These effects become stronger for larger fracture-matrix interface area, potentially providing a means for estimating this area. Previous field tests and modeling studies have demonstrated characteristic tailing in BTCs for volatile tracers in vapor-dominated reservoirs. Simulated BTCs for solute tracers in single-phase liquid systems show much weaker tails, as would be expected because diffusivities are much smaller in the aqueous than in the gas phase, by a factor of order 1000. A much stronger signal of fracture-matrix interaction can be obtained when sorbing tracers are used. We have performed simulation studies of surface-sorbing tracers by implementing a model in which the adsorbed tracer mass is assumed proportional to the fracture-matrix surface area per unit volume. The results show that sorbing tracers generate stronger tails in BTCs, corresponding to an effective enhancement of diffusion. Tailing in BTCs for sorbing tracers may provide adequate sensitivity for quantifying the fracture-matrix interface area. We discuss requirements for tracer sorption and present considerations for designing a tracer test that would determine fracture-matrix interface area.

1. INTRODUCTION

Natural and artificial tracers are important tools for determining reservoir conditions and processes. Tracer tests can provide useful information for reservoir management, and can assist in the design of production and injection operations.

This paper is concerned with water (re-)injection and the associated cooling effects. In a homogeneous porous medium, injection of colder water will give rise to a rather sharp "thermal front," where reservoir temperature changes from the temperature T_{inj} of injected water to original

reservoir temperature T_0. If hydrodynamic dispersion and the generally small effects of heat conduction in the direction of flow are neglected, it can be shown (Bodvarsson, 1972) that in a homogeneous porous medium the thermal front is mathematically "sharp," and advances with a velocity v_{th} that is related to the pore velocity v_p of a conservative (inert) solute tracer by

$$v_{th} \; = \; \frac{v_p}{R_{th}} \tag{1}$$

where the thermal retardation factor R_{th} is given by the ratio of total (rock plus fluid) heat capacity to heat capacity of the fluid

$$R_{th} \; = \; \frac{\phi \rho_w c_w + (1-\phi)\rho_R c_R}{\phi \rho_w c_w} \; = \; 1 + \frac{(1-\phi)\rho_R c_R}{\phi \rho_w c_w} \tag{2}$$

Here, ϕ is reservoir porosity, ρ is density, c is specific heat, and the subscripts w and R denote water and rock, respectively. Similarly, a tracer κ that is subject to reversible equilibrium sorption will be retarded relative to a conservative tracer, with the retardation factor given by an analogous expression

$$R^\kappa \; = \; 1 + \frac{(1-\phi)\rho_R K_d}{\phi} \tag{3}$$

that represents the ratio of total tracer inventory (dissolved plus sorbed) to tracer inventory in the fluid. The parameter K_d for sorption strength has units of specific volume (m^3/kg) and is often referred to as "distribution coefficient," as it expresses the distribution of solute between aqueous and solid phases (de Marsily, 1986).

The particular form of retardation factor given in Eqs. (2, 3) is obtained by assuming instantaneous local equilibrium between rocks and fluids, which is appropriate for homogeneous porous media. Very different behavior arises in fractured reservoirs. As cold injected water migrates through a network of fractures, heat is supplied from the fracture wall rocks by conduction. This is a slow process and gives rise to very broad temperature profiles, as opposed to the sharp fronts for homogeneous porous media (Lauwerier, 1955; Pruess and Wu, 1993; Fitzgerald et al., 1996). Thermal diffusivities of typical reservoir rocks are around 10^{-6} m^2/s, so that during a typical lifetime of a geothermal project of 30 years, the depth of conductive penetration is of the order of 30 m. This may be less than the spacing between major fluid-bearing fractures, indicating that non-equilibrium conditions and heat transfer limitations will be important effects.

In fractured reservoirs, migration velocities of conservative tracers can be large, of the order of tens of meters per hour

(Horne, 1982). For water injection, field operators generally attempt to avoid such fast, preferential pathways, as these are considered to pose a risk of premature thermal breakthrough in nearby production wells. This is a reasonable approach from a practical point of view, but it is well to remember that, strictly speaking, in fractured reservoirs there is no relationship between the migration velocities of thermal fronts and conservative solute tracers. The two processes are controlled by different physical mechanisms, and are governed by different parameters. Indeed, tracer migration is determined by the volume of the flow path between injection and production well, while the advancement of a thermal front is determined by the surface area of that flow path that is available for heat transfer (Pruess and Bodvarsson, 1984). The heat transfer area is the crucial parameter that determines rate and sustainability of energy extraction from hot fractured rock (HFR).

Tracers may allow a determination of that heat transfer area from an interplay between advective transport in fractures, and diffusive exchange with matrix rock of low permeability. The basic concept is shown in Fig. 1. As fluid containing a tracer pulse is migrating along a fracture, the concentration gradient will cause some tracer diffusion into the rock matrix. After the tracer pulse has passed the concentration gradient reverses, and tracer diffuses from the matrix back into the fracture. This back diffusion will give rise to a long tail in the tracer breakthrough curve (BTC). This tailing effect was observed for gas-phase tracers in vapor-dominated conditions (Beall et al., 1994). Modeling studies by Pruess (2002) and Shan and Pruess (2003) indicated a systematic dependence of tailing behavior on fracture spacing (or, equivalently, heat transfer area), with stronger tails for smaller fracture spacing (larger heat transfer area). Simulations presented by Pruess (2002) demonstrated that different tailing behavior observed by Beall et al. (1994) in different parts of The Geysers reservoir, California, could be interpreted in terms of different reservoir processes, namely, strong boiling in depleted reservoir zones versus weak boiling in undepleted zones.
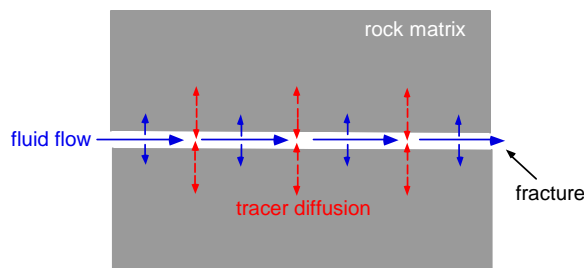

Figure 1: Interplay of fracture flow and matrix diffusion.

Application of this type of test to single-phase liquid reservoirs faces a major problem in that diffusivities of aqueous solutes are orders of magnitude smaller than gas phase diffusivities. Gas phase diffusivities under typical vapor-dominated conditions (T $\approx$ 240 °C, P $\approx$ 40 bar) are of order 10^{-6} m^2/s, very similar to thermal diffusivity, while liquid phase diffusivities are of order 10^{-9} m^2/s (Freeze and Cherry, 1979; de Marsily, 1986). Therefore, diffusive exchange with matrix rocks and resulting tails in solute tracer BTCs will be much weaker, and it may not be practically possible to use the tailing effect as a means for evaluating reservoir conditions and processes. It is the purpose of this paper to explore whether tracer testing in single-phase liquid conditions can potentially provide useful information about fracture-matrix interaction.

2. MODEL SYSTEM

We use numerical simulations to evaluate tracer BTCs for different reservoir conditions and parameters. To simplify the simulation problem we take advantage of symmetries, and assume that production and injection wells are arranged in a regular five-spot pattern (see Fig. 2). A 2-D system with a single layer of 500 m thickness was modeled, and a 5-point parallel grid (Pruess, 1991) of 196 square blocks was used to represent a 1/8 symmetry element.
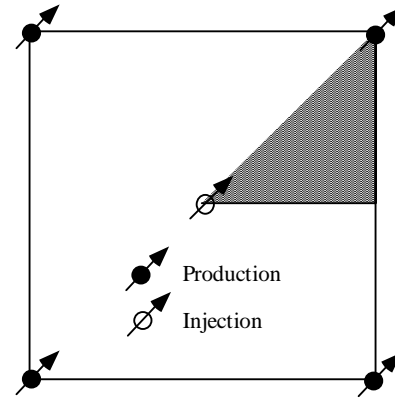

Figure 2. Five-spot well pattern, with shading showing a 1/8 symmetry element.

Some simulations were made for a 400 m x 400 m grid in which the producer-injector distance (PID) is equal to 282.8 m; for others a larger well spacing with PID = 500 m and the same number of grid blocks was used. Water is injected continuously at a rate of 64 kg/s (full-well basis) with an enthalpy of 125 kJ/kg. The production well is operated "on deliverability," which means that production rate is approximately equal to injection rate. Different scenarios have been explored for tracer testing, the most common being injection of a tracer slug of 8 hr duration at a small concentration arbitrarily chosen as 0.125 ppm. Tracer diffusivity was taken as d = 10^{-9} m^2/s in most cases, and matrix tortuosity was assumed as τ = 0.1. Problem specifications are summarized in Table 1.

Table 1. Specifications of five-spot problem

Reservoir properties	
Average permeability (of fracture network)	43.2 x10^{-15} m^2
Matrix permeability	1.9 x10^{-18} m^2
Fracture porosity	0.1 %
Matrix porosity	3 %
Thickness	500 m
Permeability-thickness	21.6 x10^{-12} m^3
Fracture spacing	2 - 100 m
Injection Rate (full well basis)	64 kg/s
Enthalpy	125 kJ/kg
Initial conditions	
Pressure	60.0 bar
Temperature	240 ÞC

It is acknowledged that a five-spot configuration is not a realistic geometric representation of typical geothermal production-injection systems. For a hot fractured reservoir, a well doublet may be a more realistic configuration. However, the geometric simplification achievable for a five-spot pattern permits a more accurate and detailed analysis of process issues, such as tracer partitioning between fractures and matrix rock, and sorption effects, and

therefore is better suited for a feasibility study such as presented here.

The reservoir is assumed to have ubiquitous fractures with some average spacing D that form a well-connected network. We idealize this situation by assuming three perpendicular fracture sets with the same uniform spacing D, so that the matrix blocks enclosed by the fractures are cube-shaped. The fracture-matrix interface area per unit reservoir volume is $a = 6D^2/D^3 = 6/D$. Our interest is primarily on the dependence of tracer BTCs on a, but the results reported in this paper are generally labeled with fracture spacing $D = 6/a$, which is a more intuitive parameter and is also used as input parameter by the TOUGH2 code employed in the simulations (Pruess et al., 1999). Fracture-matrix interactions are represented with the method of "multiple interacting continua" (MINC; Pruess and Narasimhan, 1985). Diffusive penetration into matrix blocks for time periods of interest is small, especially so when retardation effects due to sorption are included, and very fine gridding is required near the matrix block surfaces to properly resolve concentration gradients there. We have used volume fractions as small as 10^{-4} for the outermost matrix region, gradually coarsening the grid towards the interior of the matrix blocks. As many as 14 sub-continua were employed, for a total of $14 \times 196 = 2,744$ grid blocks.

For a uniformly fractured system, advancement of the thermal front is very much slower than migration of solute tracer. For the conditions considered in our study, tracer migration over the 500 m distance from injection to production well requires approximately 30 days. Our simulations were extended over a 5-year period, at the end of which the thermal front has advanced only 134.6 m away from the injection well in the most unfavorable case of smallest heat transfer area considered here (fracture spacing $D = 100$ m). The fractures in our model system are uniformly distributed; field conditions could of course be less favorable, with one or a few major extensive fractures providing preferential pathways and a more rapid thermal breakthrough.

3. NON-SORBING TRACERS

Calculations with non-sorbing tracers were done to explore different effects. Fig. 3 shows BTCs for different fracture spacing and a production-injection well spacing of PID = 500 m, and Table 2 summarizes some parameters derived from these curves. A calculation neglecting tracer diffusion was also included, to demonstrate that the tailing behavior seen in Fig. 3 is absent when diffusive exchange between fractures and matrix is suppressed. The BTC for "no
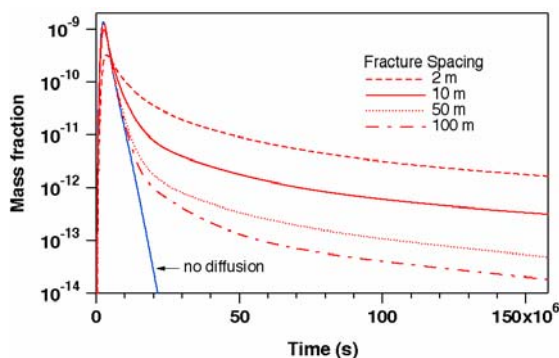

Figure 3. Tracer breakthrough curves for different fracture spacing.

Table 2. Parameters of tracer breakthrough for 500 m producer-injector distance

fracture spacing	2 m	10 m	50 m	100 m	no diffusion
peak arrival (hr)	994.4	760.7	723.0	722.8	695.2
peak concentration*	2.58e-3	7.87e-3	10.32e-3	10.73e-3	11.02e-3
relative tail concentration§	4.64e-2	4.56e-3	7.356e-4	4.195e-4	7.26e-7

* normalized to injected concentration of 0.125e-6
§ defined as concentration ratio $C(10 \times t_{peak})/C_{peak}$

diffusion" in Fig. 3 was obtained for a fracture spacing of D = 50 m, but the curve depends little on the fracture spacing chosen. For the "no diffusion" case, the peak tracer concentrations arrive at the production well at 500 m distance after 695.2 hr, corresponding to an average tracer migration velocity of 0.72 m/hr. As had been anticipated from the general mechanism of fracture-matrix interdiffusion discussed above, and from previous results for gas-phase tracers in vapor-dominated reservoirs (Pruess, 2002; Shan and Pruess, 2003), there is a systematic dependence of BTCs on fracture spacing. For smaller fracture spacing the fracture-matrix interaction becomes stronger, which delays the arrival of the concentration peak in the BTC, reduces peak concentrations, and strengthens tails in the BTCs. While the fracture-matrix exchange has dramatic effects on the tails in the BTCs, the peaks are strongly affected only when fracture spacing is reduced to small values. Peak arrival and concentration is virtually identical for fracture spacings of 50 and 100 m (Fig. 3 and Table 2).

Further insight into system behavior can be gained by examining the tracer inventory in the matrix (Fig. 4). The amount of tracer transferred to the matrix strongly increases with decreasing fracture spacing, due to the larger fracture-matrix interface area. The fraction of tracer residing in the rock matrix reaches a maximum at the time when peak concentrations arrive at the production well. The maximum tracer inventory in the matrix ranges from 6 % of total injected mass for D = 50 m to 64 % for D = 2 m. If diffusion is neglected, the only mechanism for transferring tracer into the matrix is by advection. This mechanism is active only for a relatively short time, until quasi-steady flow conditions are established, and the maximum tracer inventory in the matrix reaches a mere 1.9 % in this case.

Of most practical interest in HFR reservoir analysis are larger fracture spacings of order 50 m or more, for which fracture-matrix exchange and associated tailing effects are rather weak. As had been mentioned previously, for gas phase tracers in vapor-dominated systems, in situ diffusivities are of order 10^{-6} m^2/s. Fig. 5 shows BTCs for diffusivities ranging from values applicable for aqueous solutes to typical values for gases. Of course, these diffusivities are hypothetical; aqueous phase diffusivities are material properties of the diffusing solutes, and are typically of order 10^{-9} m^2/s at ambient temperatures, increasing by about an order of magnitude at T = 250 ˚C (de Marsily, 1986). The purpose of the simulations shown in Fig. 5 is to dramatize the challenge for utilizing fracture-matrix partitioning of tracers as a characterization tool in liquid phase conditions, where tailing effects are much weaker than in vapor-dominated conditions. It will be shown below that reversible sorption produces tailing
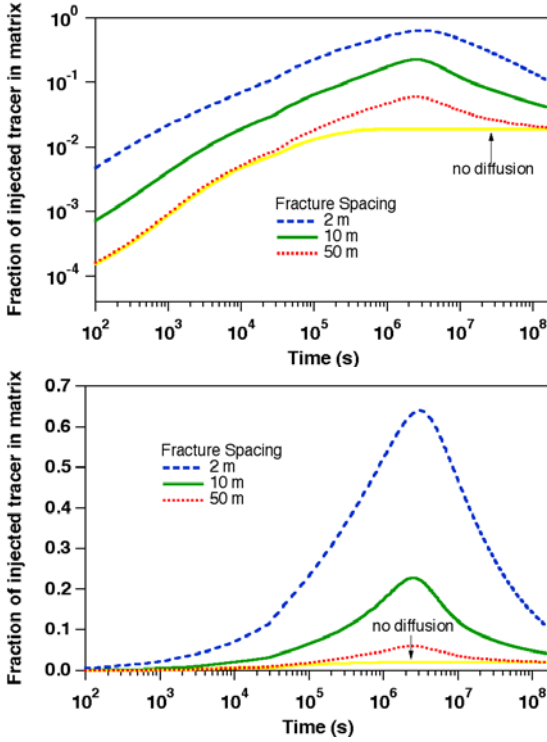
Figure 4. Fraction of injected tracer residing in the matrix on logarithmic (top) and linear scales (bottom). The "no diffusion" calculation is for D = 50 m fracture spacing.
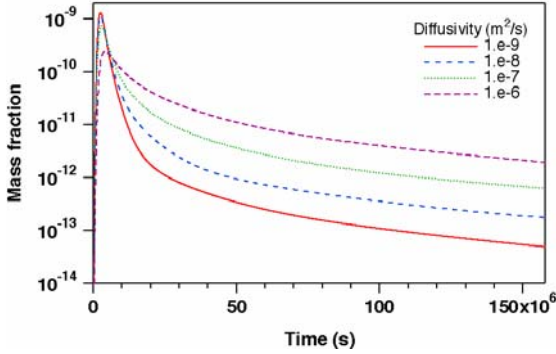

Figure 5. Tracer breakthrough curves for D = 50 m fracture spacing and a range of diffusivities.

effects that are similar to what would be obtained for increased diffusivities, so that the curves shown in Fig. 5 are not necessarily entirely hypothetical.

Different approaches may be considered for increasing the sensitivity of BTCs to larger fracture spacing. The basic challenge is to transfer a larger amount of tracer to the matrix. One way this can be accomplished is by continuing the tracer injection for a longer period of time, so that the tracer plume would contact a larger surface area of matrix blocks. Test calculations not shown here indicate that injecting for a longer period of time will indeed place more tracer in the rock matrix and increase tracer concentrations at the production well, but will not increase the fraction of tracer transferred to the rock matrix, and will not improve the tail-to-peak concentration ratios.

Another possibility we considered is to shut-in the injection after some period of time, so that the tracer would essentially stagnate in the fractures for a while, and would

have more time available to diffuse into the rock matrix. To explore this idea, we ran a case where a tracer slug was injected for 8 hours followed by solute-free water as before, but after 80 hr total time injection was shut in and was resumed after 800 hr cumulative time. The purpose was to first drive the 8 hr tracer slug out into the fracture network, then let it sit there for a while to allow diffusion to do its work and transfer more tracer to the matrix. BTCs obtained in a smaller five-spot system with 400 m x 400 m area (282.8 m producer-injector distance) are shown in Fig. 6. Curves for the case with a shut-in period are labeled "interrupted" and do show stronger tailing, as had been expected. However, most of the effect is simply due to an overall delay of BTCs by 720 hours from the shut-in period. When this delay is removed by displacing BTCs by 720 hours to the left (bottom frame in Fig. 6), the enhancement in tailing is seen to be weak, decreases with decreasing diffusivity, and is imperceptibly small for the $d = 10^{-9}$ m^2/s case.
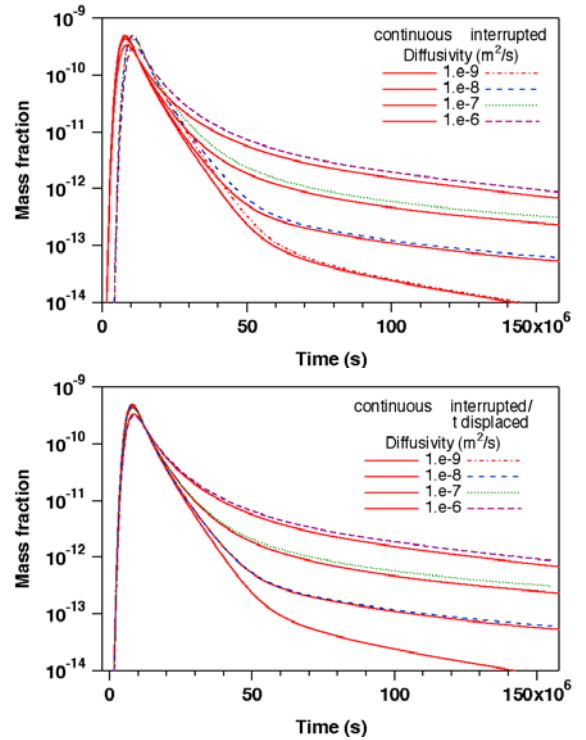

Figure 6. Breakthrough curves for continuous injection and for an "interrupted" case where injection is shut in from 80 to 800 hours. Producer-injector distance is PID = 282.8 m and fracture spacing is D = 50 m. In the bottom frame, the BTCs for the interrupted case have been displaced by 720 hours to the left, to remove the delay in arrival due to the shutin period.

4. SORBING TRACERS

Let us now consider the migration of sorbing tracers in a fractured-porous medium. Sorption occurs on mineral surfaces by cation exchange, surface complexation, and other mechanisms (de Marsily, 1986; Triay et al., 1997). A superficial analysis might suggest that the chief effect of this would be to sorb some tracer onto fracture walls, and thereby retard arrival at the production well. However, when considering sorption on the fracture walls, sorption on mineral surfaces in the matrix rock should also be included for consistency. It will be seen below that matrix sorption produces very strong effects.

We first present some considerations on the values of the distribution coefficient K_d to be used in the simulations. The fracture domain is modeled as a porous medium with 5 % intrinsic porosity, i.e., 95 % of the volume included in the fracture domain is wall rock. The rationale for including a considerable amount of wall rock into the definition of the fracture domain is discussed in Pruess (1997). The fracture domain occupies 2 % of total reservoir volume, corresponding to an overall effective fracture porosity of 0.05 x 0.02 = 0.1 %. We consider two different tracers that sorb on the fracture walls in such a way as to yield what we consider reasonable retardation factors of 1.2 and 2, respectively. For a fracture domain with porosity $\phi = 0.05$ and rock density $\rho_R = 2600$ kg/m^3, the K_d-values corresponding to these retardation factors can be calculated from Eq. (3) as 4.05×10^{-6} m^3/kg and 2.02×10^{-5} m^3/kg, respectively. For the matrix domain we assign K_d values two orders of magnitude larger, 4.05×10^{-4} m^3/kg and 2.02×10^{-3} m^3/kg, respectively. The corresponding retardation factors are 21 and 101, which are fairly large but not at all excessive. These K_d values compare favorably with K_d values in the range of 1 - 4×10^{-3} m^3/kg used by Wu et al. (2002) for sorption of neptunium in different lithologic units of the Yucca Mountain tuffs. Liu et al. (2004) measured K_d-values for cesium in sedimentary formations at the Hanford site, Washington, and found values in a wide range of from 3×10^{-3} m^3/kg to as much as 10 m^3/kg, the smaller values corresponding to regions in which cesium sorption was reduced due to the extremely high ionic strength of the aqueous phase. In a study of radionuclide migration in fractured rock, Moreno et al. (1997) examined a range of sorption coefficients. They consider a $K_d = 1/\rho_R = 3.85 \times 10^{-4}$ m^3/kg as "slightly" sorbing, while their "strongly" sorbing case corresponds to a value two orders of magnitude larger, $K_d = 3.85 \times 10^{-2}$ m^3/kg. Thus the matrix K_d values used in our simulations are within a reasonable range.

K_d-values and corresponding retardation factors in the fracture domain depend on fracture spacing as discussed in the Appendix. From the K_d-data given above for a fracture domain with D = 10 m fracture spacing, the K_d-parameters for the case with D = 50 m fracture spacing can be obtained from Eq. (A.2) as 8.10×10^{-7} m^3/kg and 4.05×10^{-6} m^3/kg, respectively. The corresponding retardation factors are 1.04 and 1.2.

Results for BTCs for 10 and 50 m fracture spacing and two different tracers with weaker and stronger sorption are shown in Figs. 7 and 8, and Table 3. Here and in what follows, all BTCs for sorbing tracers are labeled with their corresponding retardation factors in the fracture domain; matrix K_d's and associated retardation factors are the same in all cases. It is seen that sorption weakens and delays the peak while giving rise to considerably stronger tails. Retardation of peak arrivals is considerably stronger than expected from sorption on fracture walls alone (Table 3), demonstrating the strong effects from matrix sorption. BTCs for a larger diffusivity of d = 10^{-7} m^2/s were included in Figs. 7 and 8, to suggest the similarity of sorption effects to increased diffusivity. This point can be understood by considering that, in the presence of strong matrix sorption, tracer diffusing into the rock matrix will be far less effective in enhancing concentrations in the aqueous phase, due to its partitioning onto mineral surfaces. Because tracer concentrations in the aqueous phase in the matrix remain lower, concentration gradients driving tracer from the fractures to the matrix remain larger, and a larger fraction of injected tracer is transferred to the matrix. After the

tracer slug has passed, concentration gradients at the fracture-matrix interface reverse, and the sorbed inventory gives rise to stronger and more sustained backdiffusion, producing stronger tails in the BTCs.
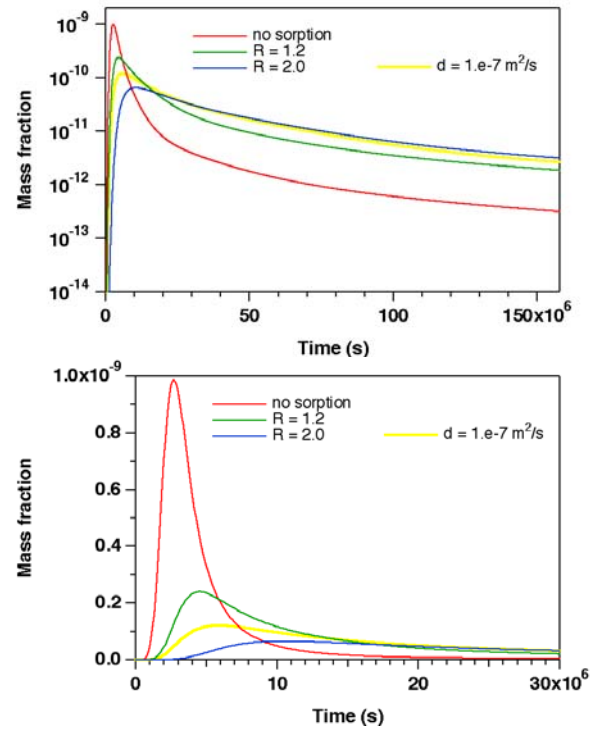

Figure 7. Breakthrough curves for sorbing tracers on logarithmic (top) and linear scales (bottom). The curves are labeled with the retardation factors in the fractures. Fracture spacing is D = 10 m.
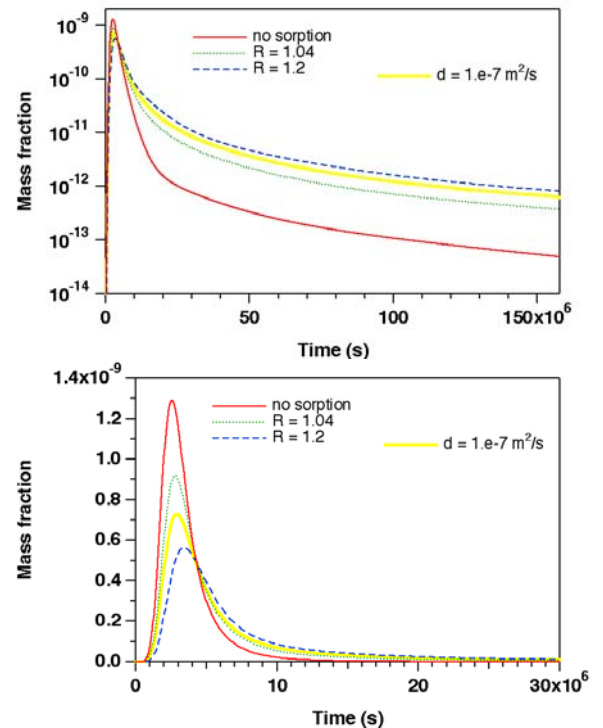

Figure 8. Breakthrough curves for sorbing tracers on logarithmic (top) and linear scales (bottom). The curves are labeled with the retardation factors in the fractures. Fracture spacing is D = 50 m.

Table 3. Sorption effects on retardation of concentration peaks.

fracture spacing	Retardation factor in fractures	simulated retardation*
10 m	1.2	1.68
10 m	2	3.91
50 m	1.04	1.08
50 m	1.2	1.34

* from peak arrival times

A more quantitative analysis can be based on an approximate analytical treatment, from which it can be shown (Luis Moreno, private communication, 2004) that the BTC for a tracer slug in a fractured-porous medium depends on rock matrix properties only through the parameter group d_e/D^2, where

$$d_e = \tau d \left[\phi + (1-\phi) \rho_R K_d \right] \qquad (4)$$

is the effective diffusivity that includes the tortuosity coefficient τ and the distribution coefficient K_d for rock matrix sorption. When sorption is neglected, the parameter group in brackets has the value $\phi = 0.03$, while for the weakly and strongly sorbing tracers used in the simulations presented in Figs. 7 and 8 the values are 1.051 and 5.135, respectively, corresponding to an effective enhancement of diffusivity by factors of 35.0 and 171.2. Fig. 9 compares BTCs for D = 50 m fracture spacing for the two cases with sorption to simulations without sorption ($K_d = 0$) but with diffusivity d enhanced such as to keep Eq. (4) invariant.
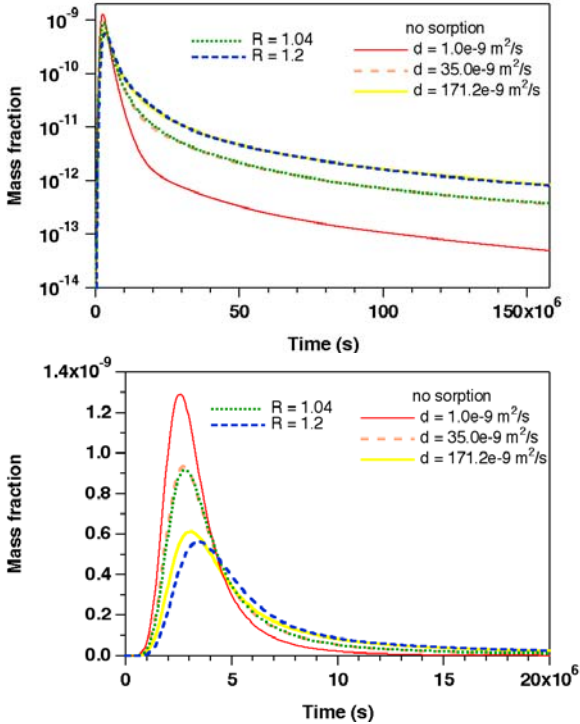

Figure 9. Breakthrough curves for sorbing tracers on logarithmic (top) and linear scales (bottom), with "no sorption" calculations with enhanced diffusivity included for comparison. The curves are labeled with the retardation factors in the fractures. Fracture spacing is D = 50 m.

The R = 1.04 case with a diffusivity of 10^{-9} m^2/s is seen to closely match the no-sorption calculation with d = 35.0×10^{-9} m^2/s. The R = 1.2 case has some differences from the no-sorption calculation with d = 171.2×10^{-9} m^2/s near the peak, but tailing behavior is virtually identical.

To test the invariance of BTCs with respect to the parameter group d_e/D^2, Fig. 10 compares simulations for d = 10^{-9} m^2/s, D = 10 m and d = 10^{-7} m^2/s, D = 100 m. The BTCs are virtually indistinguishable in the peak as well as tail regions, confirming this invariance.
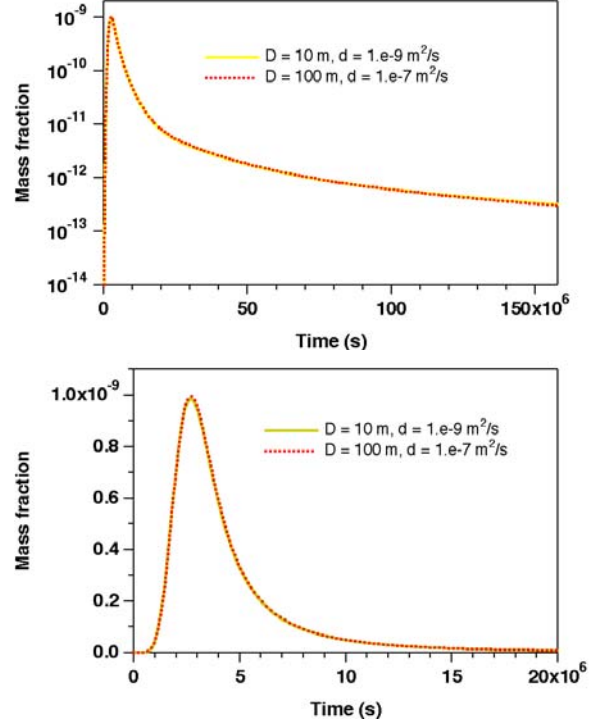

Figure 10. Breakthrough curves for non-sorbing tracers for different values of fracture spacing and diffusivity, on logarithmic (top) and linear scales (bottom).

The results presented in Figs. 9 and 10 demonstrate that in the analysis of tracer BTCs in the field, any uncertainty in tortuosity τ or distribution coefficient K_d will translate into a corresponding uncertainty of fracture spacing D.

5. DISCUSSION AND CONCLUSIONS

To be commercially sustainable, energy production from hot dry rock (HDR) and hot fractured rock (HFR) reservoirs must achieve adequate and predictable rates of heat transfer from matrix rocks of low permeability to fluids circulating in the fracture network. The crucial parameter determining the capacity and longevity of such reservoirs is the area available for heat transfer, i.e., the interface area between fractures and matrix rocks. There are currently no methods available for determining this interface area in the field. In practice, when designing production-injection operations, reservoir engineers rely on tracer tests and attempt to limit or avoid injection into wells that give rise to rapid tracer returns in neighboring production wells. This seems reasonable from a practical point of view, but it is well to remember that, strictly speaking, in a fracture network there is no correlation between the migration velocity of tracers and the rate of advancement of thermal (cooling) fronts. Indeed, tracer migration depends on the volume of the flow pathway while heat transfer depends on its surface area.

Depending on geometric shape of the flow path, vastly different surface areas may be associated with a given volume.

In order to properly design and operate HDR and HFR systems, we must not only identify and avoid short-circuiting flow paths with rapid thermal interference, we also need to be able to characterize the total heat transfer area available to the injected fluid. In this paper we have studied the feasibility of using the partitioning of solute tracers between fractures and matrix, due to molecular diffusion, as a means for determining fracture-matrix interface area in single-phase liquid reservoirs. The key feature in tracer breakthrough curves (BTCs) that may allow such a determination is the presence of long tails, induced by slow backdiffusion of tracer towards the fractures that had been transferred to the rock matrix when the tracer slug passed through the fractures.

Field studies and numerical simulations have demonstrated that such tailing may allow determination of reservoir processes, such as boiling of injectate, in vapor-dominated systems. Diffusivities of aqueous solutes are orders of magnitude smaller than diffusivities in the gas phase at typical in situ conditions. This paper has explored whether fracture-matrix exchange and associated tailing in tracer BTCs are strong enough to be practically useful in single-phase liquid systems. In the spirit of a feasibility study we have performed numerical simulations of tracer migration in a simplified model of a fractured-porous reservoir, using generic parameters for diffusivity, tortuosity, and sorptive behavior of solutes, rather than data corresponding to specific chemicals. The main findings from our simulations are as follows.

- tracer breakthrough curves in fractured-porous media have long tails that are due to solute exchange between fractures and rock matrix by molecular diffusion; when molecular diffusion is suppressed, the tails are absent;

- tailing in single-phase liquid conditions is considerably weaker than in vapor-dominated conditions, due to much smaller diffusivities in the aqueous phase as compared to gas;

- the strength of concentration tails increases systematically with decreasing fracture spacing (increasing fracture-matrix interface area);

- allowing for a quiescent period following injection of a tracer slug (shutting in injection) will increase concentrations in the tails, but the effect appears to be too small to be practically useful;

- much stronger tailing can be obtained by using sorbing tracers;

- aqueous solutes that reversibly sorb on mineral surfaces produce an effective enhancement of diffusive exchange between fractures and matrix; this is due to the fact that matrix sorption tends to keep aqueous concentrations low and concentration gradients at the fracture-matrix interface large;

- an approximate analytical treatment of tracer transport in fractured media has suggested that effects of matrix sorption and fracture spacing are tantamount to a change in effective matrix diffusivity (Luis Moreno, private communication, 2004); the invariances predicted from the analytical model were confirmed by numerical simulations;

- sorbing tracers will be sensitive not just to the fracture-matrix interface area, but of course also to the mineralogical composition and the presence of other aqueous solutes; this will complicate an unambiguous characterization of interface area;

- ambiguities in tracer BTCs may be overcome by using a cocktail of tracers with different sorbing properties.

The results of this study suggest that solutes that are subject to slight or moderately strong reversible sorption may provide useful tracers for fractured reservoirs, whose breakthrough curves can provide estimates of the fracture-matrix interface area available for heat transfer. Specific chemicals that may offer suitable properties may be found among metal cations. Design of tracer tests for specific HFR systems will require laboratory experiments, using crushed reservoir rocks and reservoir brines, to determine K_d values and select appropriate sorbing solutes suitable for a field test.

ACKNOWLEDGEMENT

REFERENCES

Beall, J.J., M.C. Adams and P.N. Hirtz. R-13 Tracing of Injection in The Geysers, *Transactions,* Geothermal Resources Council, Vol. 18, pp. 151 - 159, 1994.

Bodvarsson, G. Thermal Problems in the Siting of Reinjection Wells, *Geothermics*, Vol. 1, No. 2, pp. 63 - 66, 1972.

de Marsily, G. *Quantitative Hydrogeology*, Academic Press, Orlando, FL, 1986.

Fitzgerald, S.D., C.T. Wang and K. Pruess. Laboratory and Theoretical Studies of Injection into Horizontal Fractures, Proceedings, 18th New Zealand Geothermal Workshop, pp. 267 - 273, Auckland, New Zealand, September 1996.

Freeze, R. A. and J. A. Cherry. *Groundwater*, Prentice-Hall, Inc., Englewood Cliffs, NJ, 1979.

Horne, R. Geothermal Reinjection Experience in Japan, *J. Petr. Tech.*, pp. 495 - 503, March 1982.

Lauwerier, H.A. The Transport of Heat in an Oil Layer Caused by the Injection of Hot Fluid, *Appl. Sci. Res.*, 5, Section A (2-3), 145-150, 1955.

Liu, C., J.M. Zachara and S.C. Smith. A Cation Exchange Model to Describe Cs^+ Sorption at High Ionic Strength in Subsurface Sediments at Hanford Site, USA, *J. Contam. Hydr.,* Vol. 68, Nos. 3-4, pp. 217 - 238, 2004.

Moreno, L., B. Gylling and I. Neretnieks. Solute Transport in Fractured Media - the Important Mechanisms for

Performance Assessment, *J. Contam. Hydr.,* Vol. 25, pp. 283 - 298, 1997.

Pruess, K. Grid Orientation and Capillary Pressure Effects in the Simulation of Water Injection into Depleted Vapor Zones, *Geothermics,* Vol. 20, No. 5/6, pp. 257 - 277, 1991.

Pruess, K. On Vaporizing Water Flow in Hot Sub-Vertical Rock Fractures, *Transport in Porous Media,* Vol. 28, pp. 335 - 372, 1997.

Pruess, K. Numerical Simulation of Multiphase Tracer Transport in Fractured Geothermal Reservoirs, *Geothermics,* Vol. 31, pp. 475 - 499, 2002.

Pruess, K. and G.S. Bodvarsson. Thermal Effects of Reinjection in Geothermal Reservoirs with Major Vertical Fractures, *J. Pet. Tech.,* 36 (10), 1567–1578, 1984.

Pruess, K. and T.N. Narasimhan. A Practical Method for Modeling Fluid and Heat Flow in Fractured Porous Media, *Soc. Pet. Eng. J.,* 25 (1), 14-26, February 1985.

Pruess, K. and Y. S. Wu. A New Semianalytical Method for Numerical Simulation of Fluid and Heat Flow in Fractured Reservoirs, *SPE Advanced Technology Series,* Vol. 1, No. 2, pp. 63-72, 1993.

Pruess, K., C. Oldenburg and G. Moridis. TOUGH2 User's Guide, Version 2.0, Lawrence Berkeley National Laboratory Report LBNL-43134, Berkeley, CA, November 1999.

Shan, C. and K. Pruess. Numerical Simulation of Noble Gases as Natural Tracers for Injection Returns and Reservoir Processes in Vapor-Dominated Systems, Proceedings, 28th Workshop on Geothermal Reservoir Engineering, report SGP-TR-173, Stanford University, Stanford, CA, January 2003.

Triay, I.R., A. Meijer, J.L. Conca, K.S. Kung, R.S. Rundberg, B.A. Strietelmeier and C.D. Tait. Summary and Synthesis Report on Radionuclide Retardation for the Yucca Mountain Site Characterization Project, Los Alamos National Laboratory Report LA-13262-MS, Los Alamos, NM, March 1997.

Wu, Y.S., L. Pan, W. Zhang and G.S. Bodvarsson. Characterization of Flow and Transport Processes within the Unsaturated Zone of Yucca Mountain, Nevada, Under Current and Future Climates, *J. Contam. Hydr.,* Vol. 54, pp. 215 - 247, 2002.

APPENDIX: TREATMENT OF SURFACE-SORBING TRACERS

Consider a single-phase liquid reservoir with a solute tracer κ that is subject to linear reversible equilibrium sorption. Tracer inventory per unit volume is given by

$$M^{\kappa} \;=\; \phi \rho_w X_w^{\kappa} + (1-\phi)\rho_R \rho_w X_w^{\kappa} K_d$$

(A.1)

where ϕ is porosity, ρ is density, X^{κ} is tracer mass fraction, and the subscripts w and R denote water and rock, respectively. As is customary, the adsorbed mass in Eq. (A.1) is written as product of the bulk dry density of the porous medium $((1-\phi)\rho_R)$, the solute concentration $(\rho_w X_w^{\kappa})$, and a strength coefficient K_d (Freeze and Cherry, 1979). Sorption is actually occurring on rock grain surfaces, so should be proportional to total rock surface area per unit volume. Eq. (A.1) can be re-interpreted in this fashion by introducing k_d, the sorption strength coefficient per unit area. To obtain the sorption coefficient per unit volume, k_d needs to be multiplied with a_V, the rock surface area per unit volume,

$$K_d \;=\; k_d a_V$$

(A.2)

k_d may be considered a material constant, that depends on mineralogical composition, grain sizes and shapes, etc., and would be the same in fractures and matrix (unless fracture walls have different mineral composition with different sorptive properties). Generally speaking, k_d may also depend on thermodynamic conditions (temperature, pressure, and composition of the aqueous phase).

In a fractured reservoir, the fraction of matrix volume is $(1 - v_f)$, where v_f is the volume fraction of fractures, a generally small number of order 1 %. Let us consider cubic matrix blocks. For fracture spacing D, matrix block size is D' with $(D')^3 = (1 - v_f)D^3$. Total fracture surface area per unit volume is

$$a_V \;=\; 6(D')^2 \big/ (D')^3 \;=\; 6/D' \;=\; \frac{6}{D(1-v_f)^{1/3}} \;\approx\; 6/D$$

(A.3)

Introducing Eqs. (A.2, 3) into Eq. (3), the retardation factor due to sorption on fracture surfaces can be written

$$R^{\kappa} \;=\; 1 + \frac{(1-\phi)\rho_R (6k_d)}{\phi D}$$

(A.4)